World Journal of Applied Physics
2016; 1(2): 48-58
http://www.sciencepublishinggroup.com/j/wjap
doi: 10.11648/j.wjap.20160102.14

Calculation of Scattering Magnetic Fields, Arising at Current Flow Around Defects, as Applied to Electromagnetic Non-destructive Testing

Yurii I. Dzhezherya[1, *], Maxim V. Sorokin[2], Victor V. Lepekha[1], Serhii V. Cherepov[1]

[1]Institute of Magnetism, National Academy of Sciences of Ukraine and Ministry of Education and Science of Ukraine, Vernadsky Blvd, Kyiv, Ukraine

[2]Institute of Mathematical Machines and Systems Problems, National Academy of Sciences of Ukraine, Glushkova Ave, Kyiv, Ukraine

Email address:
dui_kpi@ukr.net (Y. I. Dzhezherya)
[*]Corresponding author

To cite this article:
Yurii I. Dzhezherya, Maxim V. Sorokin, Victor V. Lepekha, Serhii V. Cherepov. Calculation of Scattering Magnetic Fields, Arising at Current Flow Around Defects, as Applied to Electromagnetic Non-destructive Testing. *World Journal of Applied Physics.* Vol. 1, No. 2, 2016, pp. 48-58. doi: 10.11648/j.wjap.20160102.14

Received: September 13, 2016; **Accepted**: November 14, 2016; **Published**: December 16, 2016

Abstract: The aim of the electromagnetic non-destructive testing is the determination of structural defects in conductive materials by excitation of eddy-currents using an external alternating magnetic field and measuring a secondary field produced by these currents. For a reliable control of defects in a conductor it is necessary to find out how a certain form of defect distorts the primary magnetic field. For this purpose, we use the method of approximate calculation of the distribution of magnetic fields arising at eddy-currents flow around defects of a conductor. We consider the approximation when the thickness of a skin layer is much greater than the sizes of the defect. In this case the problem of determining the scattering fields splits into two independent stages. Initially the distribution of currents in the vicinity of the defect is determined. This stage is reduced to the Neumann problem for the Laplace equation. At the second stage the restore of the magnetic field using the found currents is performed. In the framework of the method two problems were resolved: we obtained the distributions of the magnetic field at current flow around surface defects in the form of a hemisphere and half of an oblate spheroid.

Keywords: Eddy-Current Non-destructive Testing, Electromagnetic Non-destructive Testing, Eddy-Currents, Current Distribution, Magnetic Field Distribution

1. Introduction

The electromagnetic or eddy-current non-destructive testing is one of the most widely used methods for detection of defects in metal products (especially in weak-magnetic metals) [1-6]. This method is based on the excitation of induction currents in the controlled area of the sample by using an alternating magnetic field (MF) and measuring a secondary field generated by these currents. Taking into account the measured signal (for instance, using an electro-moving force induced by induction currents fields in the receiving coil), we can conclude whether any defects are presented in this area. Usually a signal from the controlled area compares with a signal from the area containing no defects.

To obtain a reliable information on the size of the defect, its shape and depth it is necessary to compare the topography (distribution) of MF, created by induced currents over the area of the sample containing no defects, with that one over the area with defect.

The definition of MF topography in the area of the defect with a predetermined configuration is the goal of the present study. From the point of view of electrodynamics this is a problem of the finding the distribution of the electromagnetic field (EMF) in the system of conductors and insulators neighboring with each other for given external field sources.

The fields are determined by solving the Maxwell's equations [7, 8] customized for each of the media:

$$\operatorname{rot}\mathbf{E} = -\frac{1}{c}\frac{\partial \mathbf{B}}{\partial t} \tag{1a}$$

$$\operatorname{rot}\mathbf{H} = \frac{1}{c}\frac{\partial \mathbf{D}}{\partial t} + \frac{4\pi}{c}\left(\mathbf{j}_e + \mathbf{j}\right) \tag{1b}$$

$$\operatorname{div}\mathbf{B} = 0 \tag{1c}$$

$$\operatorname{div}\mathbf{D} = 4\pi\rho_e \tag{1d}$$

Subject to conditions at the interfaces between the dielectric and conducting media we have

$$B_{1n} = B_{2n},\ H_{1\tau} = H_{2\tau},\ E_{1\tau} = E_{2\tau} = 0,\quad D_{1n} = D_{2n} = 0 \tag{2}$$

Here the indices 1 and 2 refer to the 1st and 2nd adjoining media, index n refers to the component of the corresponding vector which is normal to the interface, and the index τ – to the tangential component, and also the material equations relating the stress vectors $\mathbf{E}$, $\mathbf{H}$ and the induction of the electric and magnetic fields, correspondingly: $\mathbf{D}(\mathbf{E})$, $\mathbf{B}(\mathbf{H})$. Here ρ_e is the density of the external charges (hereinafter $\rho_e = 0$), $\mathbf{j}_e$ and $\mathbf{j}$ are the current densities: $\mathbf{j}_e$ corresponds to the external sources of EMF, $\mathbf{j}$ – to the induction one.

This problem is difficult for analytical investigation and not always can be solved exactly, even when the boundaries between the media and the field sources have a simple form.

Therefore certain simplifications in the formulation of the problem are required basing on the practical demands of non-destructive testing.

2. Quasi-stationary Approximation

Since high frequency EMP penetrate into the conductor to a small depth, the fields whose frequency does not exceed a few hundred kilohertz are used for non-destructive testing. The range of frequencies used is limited from below to about a hundred Hz to avoid interference from household appliances, operating at frequencies of $50-60$ Hz.

We assume that the size of the defect is significantly less than the characteristic distances over which the magnetic field created by an external source significantly changes. This situation is easily realized in practice, for example, to a low-frequency magnetic field at a great distance from the source of the field or when the size of the source is much greater than the size of the defect. In this case, we can consider a fragment of a sample with a defect like staying in a uniform external field (Fig. 1). We assume that the parameters of the system satisfy the following conditions:

$$z_0, d << \lambda$$

where z_0 is the depth of the defect, d is the defect size, λ is the characteristic scale of the magnetic field variation. As already mentioned, the parameter λ is specified by the sizes of the field source or by the distance between it and the location of the defect.

As shown in Fig. 1, the Oy axis in the area of the defect is selected in parallel to the external field.

To calculate the EMF with frequencies $0.1-100$ kHz, we can use the Maxwell's equations in the quasi-stationary approximation [7, 8], which is as follows. If the characteristic time T of EMF changes significantly exceeds the propagation time of the field, i.e., $T >> l/c$, in other words, the wavelength λ of the EMF is much larger than the system size l, i.e., $\lambda >> l$, the time derivatives in Eqs. (1) are significantly less than the space ones. Therefore, in calculation of the fields in the quasi-stationary approximation it is reasonable to neglect the displacement current $(1/c)\cdot\dot{\mathbf{D}}$ in Eq. (1b) (the dot here and below denotes the derivative with respect to time). It is necessary to leave the time derivative in (1a) otherwise the relation between changes in the electric and magnetic fields is lost.

The quasi-stationary approximation is further basis for calculating the EMF.

Next, we assume that the medium under consideration are linear and isotropic, i.e., the material equations are written in the simplest way:

$$\mathbf{D} = \varepsilon\mathbf{E},\ \mathbf{B} = \mu\mathbf{H} \tag{3}$$

where ε and μ are the permittivity and magnetic permeability of the media, correspondingly. The conductors obey the Ohm's law and have a constant conductivity σ:

$$\mathbf{j} = \sigma\mathbf{E} \tag{4}$$

As periodic established EMFs are used for non-destructive testing, let us make one more simplification. We assume that the dependences of the external current, and hence the electric and magnetic fields, on time are strictly harmonic:

$$\mathbf{j}_e,\ \mathbf{E},\ \mathbf{H} \sim \exp(i\omega t)$$

Accordingly, in the equations the dependence of these quantities on time will appear instead of the time derivative of the factor $i\omega$ in front of the corresponding value, for example, $\dot{\mathbf{E}} = i\omega\mathbf{E}$.

The induced currents in the conductor are also subject to certain equations similar to those of EMF [8]:

$$\Delta\mathbf{j} - \frac{4\pi\mu\sigma}{c^2}\frac{\partial\mathbf{j}}{\partial t} = 0 \tag{5}$$

The boundary conditions for the currents are clear: the current component normal to the boundary of the conductor should be equal to zero:

$$j_n\big|_S = 0 \tag{6}$$

When the external current $\mathbf{j}_e$ is time dependent harmonically, then Eq. (5) has the form of the Helmholtz equation

$$\Delta\mathbf{j} + k^2\,\mathbf{j} = 0 \tag{7}$$

with an imaginary coefficient

$$k^2 = -i\frac{4\pi\mu\sigma\omega}{c^2} = \left(\frac{1-i}{\delta}\right)^2,\ \delta = \frac{c}{\sqrt{2\pi\mu\sigma\omega}} \tag{8}$$

The parameter δ has the dimension of length and is a measure of the penetration of a variable EMF in the conductor. (The concentration of a variable EMF near the surface of the conductor is called skin effect, and δ is the skin depth [7, 8].) It is evident that the penetration depth depends on the conductivity and permeability of the material and, as already noted, on the frequency of EMF.

The latter circumstance is essential for non-destructive testing. Firstly, the internal defects occurring at different depths, while changing the frequency of the primary field should likely produce a different contribution to the induced EMF, and based on this can be found. Secondly, the signal from the surface defect must depend on the relation between the frequency of EMF and depth of the defect. By means of it the depth of the defect can be estimated.

These assumptions provide an important reason to consider the problem of finding the distribution of the induced EMF at an arbitrary frequency of the primary field ω or the depth of the skin layer δ.

However, in its solving the substantial mathematical difficulties associated with the need to solve various equations for dielectric and conductor, and then "sew" the solutions using the boundary conditions (2), arise.

The situation is considerably simplified in the limit of high and low frequencies. The small those at which the skin depth is much greater than the linear size d of the defect or its depth h : $\delta \gg \max\{d,h\}$. The large frequencies are corresponded to the inverse conditions, $\delta \ll \max\{d,h\}$.

These limiting cases are interesting both by themselves and from the point of view of determining the qualitative nature of the distribution of EMF above the defect, if at an arbitrary skin depth the obtaining of an analytical solution is impossible. A possible interest also related with the fact that at numerical solution of the problem it is necessary to check the computational model and the selected numerical method on the problem for which the analytical solution is known.

Let us consider the first limiting case in more detail.

3. The Method of Approximate Calculation of Magnetic Field Distribution at a Great Depth of the Field Penetration

Since at the non-destructive testing of a sample the signals from the defect-free region and from the region containing the defect are compared, we will be interested, first of all, in the supplement to the MF associated with the presence of the defect, which we will call a scattering field.

Let us calculate the scattering fields generated at induction current flow around defects of a simple form in the limit of a large depth of the skin effect.

In this case, the induced current in a conductor assumed to be homogeneous far from the defect. Moreover, if the area of the sample with the induced currents have cross-sectional dimensions much larger than d (that is technically easy to implement), then it is possible to reduce the problem to the following simple form.

Far from the defect we have a uniform current $\mathbf{j}_0$. It is necessary to find current changes $\mathbf{j}(\mathbf{r})$ caused by a defect, and then calculate the MF by the Biot-Savart-Laplace's law:

$$\mathbf{H} = \frac{1}{c}\int_{V_1} dV' \frac{\left[\mathbf{j}(\mathbf{r}')\times(\mathbf{r}-\mathbf{r}')\right]}{\left|\mathbf{r}-\mathbf{r}'\right|^3} \tag{9}$$

Here $\mathbf{r}$ and $\mathbf{r}'$ are the radius vectors of the observation point and the integration volume element, correspondingly. The integration is performed over the entire volume of the conductor V_1.

To solve this problem we should know the explicit form of the function $\mathbf{j}(\mathbf{r})$.

In the first approximation by the small parameter d/δ the distribution of the induced current $\mathbf{j}(\mathbf{r})$ does not depend on frequency and is described by the same equations as the distribution of direct current [7, 8]:

$$\operatorname{div}\mathbf{j} = 0,\ \operatorname{rot}\mathbf{j} = 0 \tag{10}$$

The fact that it is variable will be expressed with the help of a multiplier $\exp(i\omega t)$.

Only the shape of the boundary surfaces of the conductor and defect affects the particular type of $\mathbf{j}(\mathbf{r})$. This is reflected in the accounting of boundary conditions (6) for the solution of Eq. (10).

In solving of Eq. (10) one should also take into account that at the distance from the defect the current becomes uniform:

$$\mathbf{j}(\mathbf{r}\to\infty) = \mathbf{j}_0 \tag{11}$$

Using a potential character of $\mathbf{j}(\mathbf{r})$ ($\operatorname{rot}\mathbf{j} = 0$), we can introduce a current potential φ in a standard way:

$$\mathbf{j} = \operatorname{grad}\varphi \tag{12}$$

and reformulate the problem of finding the current distribution for the potential $\varphi(\mathbf{r})$ as follows:

$$\Delta\varphi = 0 \tag{13}$$

$$\left.\frac{\partial\varphi}{\partial n}\right|_S = 0,\ \varphi(\mathbf{r}\to\infty)\to\varphi_0 = \mathbf{j}_0\mathbf{r}$$

where $\partial/\partial n$ denotes the derivative with respect to the normal to the surface of the conductor, φ_0 is the potential of a uniform current.

In the form of (13) the problem under consideration is the

Neumann's problem for the Laplace equation, and the mathematical formalism of its solving is a well-developed [9, 10].

The MF defined by (9) is not yet a scattering field, it is a complete MF outside the conductor. Let us select from it just that component, which is due to a current flow around the defect.

Without a defect, the current would be uniform $\mathbf{j}(\mathbf{r}) = \mathbf{j}_0$ in the whole conductor, and the field outside the conductor would be equal to

$$\mathbf{H}_0 = \frac{1}{c} \int\limits_{V_1+V_2} dV' \frac{\left[\mathbf{j}_0 \times (\mathbf{r}-\mathbf{r}')\right]}{|\mathbf{r}-\mathbf{r}'|^3} \quad (14)$$

where V_2 is the volume of the defect.

The presence of the defect distorts the current distribution, so that in its vicinity we have

$$\varphi(\mathbf{r}) = \mathbf{j}_0\mathbf{r} + \delta\varphi(\mathbf{r}),\ \mathbf{j}(\mathbf{r}) = \mathbf{j}_0 + \delta\mathbf{j}(\mathbf{r}) \quad (15)$$

The components $\delta\mathbf{j}(\mathbf{r})$ and $\delta\phi(\mathbf{r})$ satisfy the same equations as functions $\mathbf{j}(\mathbf{r})$ and $\phi(\mathbf{r})$, however, for other conditions far from the defect and on the surface of the conductor, for example:

$$\Delta\delta\varphi = 0 \quad (16)$$

$$\left.\frac{\partial\delta\varphi}{\partial n}\right|_S = 0,\ \delta\varphi(\mathbf{r}\to\infty)\to 0$$

The difference between the MFs of the conductor with and without defect represents the scattering field $\delta\mathbf{H} = \mathbf{H} - \mathbf{H}_0$:

$$\delta\mathbf{H} = -\frac{1}{c}\int\limits_{V_2} dV' \frac{\left[\mathbf{j}_0 \times (\mathbf{r}-\mathbf{r}')\right]}{|\mathbf{r}-\mathbf{r}'|^3} + \frac{1}{c}\int\limits_{V_1} dV' \frac{\left[\delta\mathbf{j}(\mathbf{r}') \times (\mathbf{r}-\mathbf{r}')\right]}{|\mathbf{r}-\mathbf{r}'|^3} \quad (17)$$

Here in the first term the integration is performed over the volume of the defect, in the second term – over the volume of a conductor.

The calculation of the scattering field, instead of calculating the total MF, has a significant advantage because its distribution gives a picture of the currents MF distortion by a defect.

This is especially convenient for comparison with an experiment, as when performing the measurements in the field of eddy-current non-destructive testing it is important to extract a signal induced by a defect using either differential, compensation methods, or the fact that the field due to a defect has a direction different from the field induced over the defect-free area.

In addition, the scattering field is more convenient to calculate both analytically and numerically.

For example, the influence of the surfaces of a conductor which are distant from the defect on the current distribution near the defect is negligible. To exclude it from a consideration, one can imagine that the conductor occupies infinitely large area, such as half-space. In this case the integrals over the volume of a conductor in (9) are divergent because their integrands do not vanish at infinity. On the contrary, the integrals over the volume of a conductor in the expression for a scattering field (17) give the finite values because the components to the current or potential vanish at infinity.

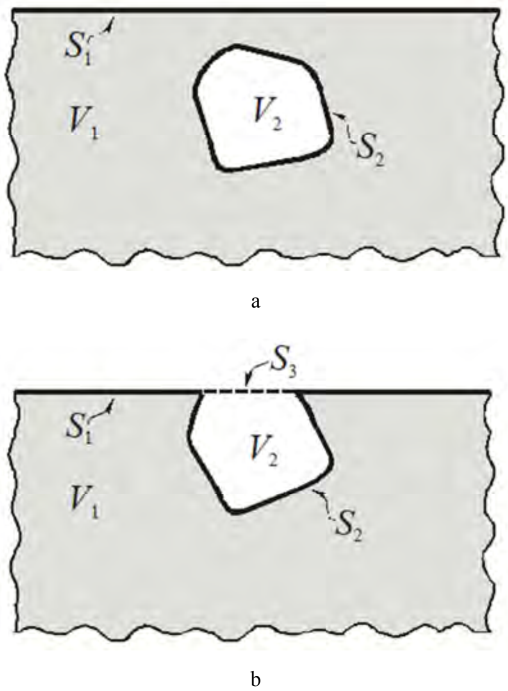

Fig. 1. *Internal defect (a) and surface defect (b).*

Using the Gauss' theorem let us rewrite the expression for a scattering MF in the form that contains only the surface integrals, and therefore has an advantage at the numerical analysis:

$$\delta\mathbf{H} = -\frac{1}{c}\mathbf{j}_0 \times \oint\limits_{S_2^+ + S_3} d\mathbf{S}' \frac{1}{|\mathbf{r}-\mathbf{r}'|} - \frac{1}{c}\int\limits_{S_1+S_2^-} d\mathbf{S}' \times \frac{\delta\mathbf{j}(\mathbf{r}')}{|\mathbf{r}-\mathbf{r}'|} \quad (18)$$

Here S_3 is the surface which "closes" the defect. Respectively, if the defect is internal (Fig.1a), the integration in the first integral is carried out only on S_2. Further, in (18) it should be taken into account that at integration over the surface of the defect S_2, the vectors $d\mathbf{S}'$ in the first term and in the second one should be oppositely directed. Respectively, S_2^+ denotes the case when the normal to the surface of the defect is directed outwards, S_2^- – inside the defect.

Before turning to the specific calculations, we note that all the obtained results can be used also in relation to the current non-destructive testing when direct or alternating current is passed directly to the test sample [11].

Now, when the mathematical aspect of the study is specified, let us consider a number of problems on the current flow, which is uniform at infinity, around single defects of a simple form in semi-infinite conductor.

4. Surface Defect in the Form of a Hemispherical Recess

We begin with a surface defect in the form of a hemisphere in a conductor with a flat surface occupying a half-space. We choose a Cartesian coordinate system with the origin at the center of the base of the hemisphere and with *Oz* axis perpendicular to the surface of a conductor. The *Ox* axis is directed along the current at infinity (Fig. 2).

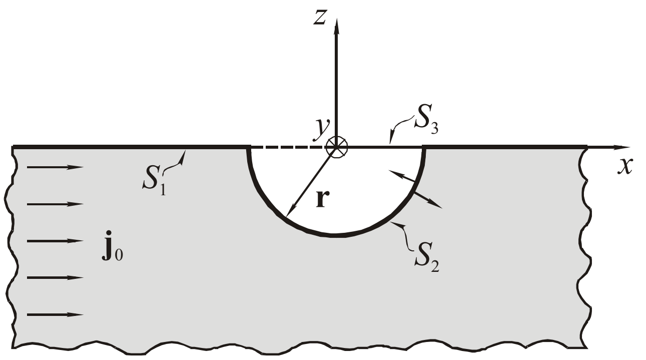

Fig. 2. *Surface defect in the form of a hemispherical recess.*

To find the distribution of $\mathbf{j}(\mathbf{r})$ the equation for the current or potential, together with the boundary conditions on the flat surface of a conductor and on the surface of a hemisphere, should be solved.

This problem is fully equivalent to finding the velocity field at the potential flow of a body of corresponding form by inviscid incompressible fluid [12-14].

Its solution for a sphere is well known [12-14]. For the boundary surface in the form of a plane with a hemispherical convex it should have the same form. This is obvious, since on the plane passing through the center of a sphere and parallel to the velocity of fluid at infinity the condition of zero normal velocity component is fulfilled automatically by symmetry:

$$\mathbf{j} = \mathbf{j}_0 + \delta\mathbf{j} = \mathbf{j}_0 + \frac{1}{2}\left[\mathbf{j}_0 r^2 - 3(\mathbf{j}_0\mathbf{r})\mathbf{r}\right]\frac{R^3}{r^5} \tag{19}$$

To find the field, let us substitute (19) into (18) taking into account that $\mathbf{j}_0 = j_0\,\mathbf{e}_x$, $d\mathbf{S}' = \mathbf{e}_z dS'$ for S_1 and S_3, $d\mathbf{S}' = \pm\mathbf{n}' dS'$, $r' = R$ for $S_2^{\pm}$, $\mathbf{n}' = \mathbf{r}'/r'$. As a result, we obtain

$$\frac{c}{j_0}\cdot\delta\mathbf{H} = -\frac{3}{2}\int\limits_{S_2^+} dS'\left[\mathbf{e}_x\times\mathbf{n}'\right]\frac{1}{|\mathbf{r}-\mathbf{r}'|} + \mathbf{e}_y\int\limits_{S_3} dS'\,\frac{1}{|\mathbf{r}-\mathbf{r}'|} - \\ -\int\limits_{S_1} dS'\left[\mathbf{e}_z\times\left(\frac{1}{2}\mathbf{e}_x r'^2 - \frac{3}{2}x'\mathbf{r}'\right)\right]\frac{R^3}{r'^5}\frac{1}{|\mathbf{r}-\mathbf{r}'|} \tag{20}$$

Each of the integrals in (20) in the spherical coordinate system

$$\mathbf{r} = (r\sin\theta\cos\alpha,\ r\sin\theta\sin\alpha,\ r\cos\theta)$$

where $0 \le r < \infty$, $0 \le \theta \le \pi/2$, $0 \le \alpha \le 2\pi$, is a particular case of the integrals of the form

$$F(\mathbf{r}) = \int\limits_{r_1}^{r_2} dr'\int\limits_{\theta_1}^{\theta_2} d\theta'\int\limits_{\alpha_1}^{\alpha_2} d\alpha'\,\frac{f_1(r')f_2(\theta')f_3(\alpha')}{|\mathbf{r}-\mathbf{r}'|}$$

It is difficult to calculate them analytically, but it is possible to obtain an approximate result using the inverse distance decomposition in spherical harmonics:

$$\frac{1}{|\mathbf{r}-\mathbf{r}'|} = \sum_n^{\infty}\sum_{m=-n}^{n}\frac{(n-|m|)!}{(n+|m|)!}\frac{r'^n}{r^{n+1}}P_{nm}(\cos\theta)P_{nm}(\cos\theta')e^{im\alpha}e^{-im\alpha'} \quad \text{for} \quad r > r'$$

where $P_{nm}(\cos\theta)$ are the associated Legendre polynomials [9, 10].

Then the corresponding integrals shall be expressed by a double sum on m and n, in each term of which the integration with respect to the groups of variables α', θ' and r' will be performed independently.

Thus, as a result of integration, we obtain the expansion of the field components in a series of spherical harmonics, each of which satisfies the Laplace equation.

By the described above trivial, but rather cumbersome transformations, we obtain the following expressions for the components of MF:

$$\delta H_x(\mathbf{r}) = -3\pi\frac{j_0}{c}\frac{R^3}{r^2}\sin\alpha\cos\alpha\cdot\sum_{n=2}^{\infty}\frac{P_{n2}(0)}{(n+2)(n-1)^2 n(n+1)}\left(\frac{2n+1}{n+2} - \frac{R^{n-1}}{r^{n-1}}\right)P_{n2}(\cos\theta),\ r > R \tag{21}$$

$$\delta H_y(\mathbf{r}) = \pi\frac{j_0}{c}\frac{R^3}{r^2}\left(\cos(\theta) - \frac{1}{4}\right) + \frac{3}{2}\pi\frac{j_0}{c}\frac{R^3}{r^2}\cdot\sum_{n=2}^{\infty}\frac{n\cdot P_n(0)}{(n-1)(n+2)}\left(\frac{2n+1}{3\cdot n} + \frac{R^{n-1}}{r^{n-1}}\right)P_n(\cos\theta) + \\ + \frac{3}{2}\pi\frac{j_0}{c}\frac{R^3}{r^2}\cos(2\alpha)\cdot\sum_{n=2}^{\infty}\frac{P_{n2}(0)}{(n-1)^2 n(n+1)(n+2)}\left(\frac{2n+1}{n+2} - \frac{R^{n-1}}{r^{n-1}}\right)P_{n2}(\cos\theta),\ r > R \tag{22}$$

$$\delta H_z(\mathbf{r}) = -\pi\frac{j_0}{c}\cdot\frac{R^3}{r^2}\sin\theta\sin\alpha - 3\pi\frac{j_0}{c}\cdot\frac{R^2}{r}\sin\alpha\cdot\sum_{n=2}^{\infty}\frac{P_n(0)}{(n+2)(n-1)}\frac{R^n}{r^n}P_{n1}(\cos\theta),\ r > R \tag{23}$$

Basing on these relations we come to the following conclusions which are of particular interest in non-destructive testing.

First, the scattering MF decreases sufficiently rapidly with a distance from the defect as $1/r^2$ at large distances ($r >> R$). Second, the principal terms of the expansion of MF are proportional to R^3 , i.e., to the volume of defects.

The dependence of the scattering field components δH_x , δH_y , δH_z on coordinates in the plane of a sample, which is just scanned for non-destructive testing, is shown in Fig. 3.

Let us compare the results obtained analytically with experimental data.

In works [15, 16] (see also [2]) the peculiarities of the topography of the magnetic field on the surface defects such as a gap, flown by a direct current or alternating current, in plane non-magnetic and ferromagnetic samples were studied. The investigations were conducted on slabs of 13-15 mm thickness with large transverse dimensions. The sizes of gaps were ranged within the following limits: width of 0.5 mm, depth of 2-13 mm, and length of 7.5-60 mm. The density values of a direct current and alternating current were equal to $j = 20\,\mathrm{A/sm^2}$. For all measurements the current was directed perpendicular to the long side of a gap. The measurements of the defects' field in the plates were performed by the fluxgate method.

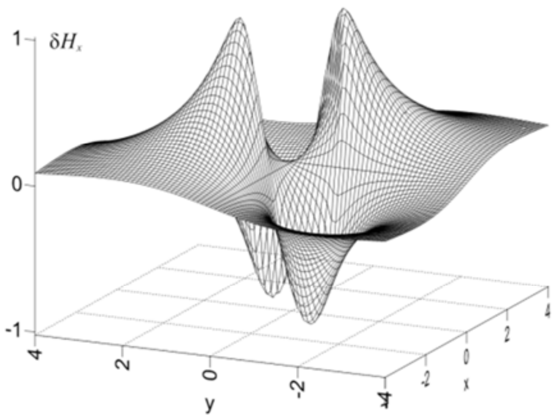

(a)

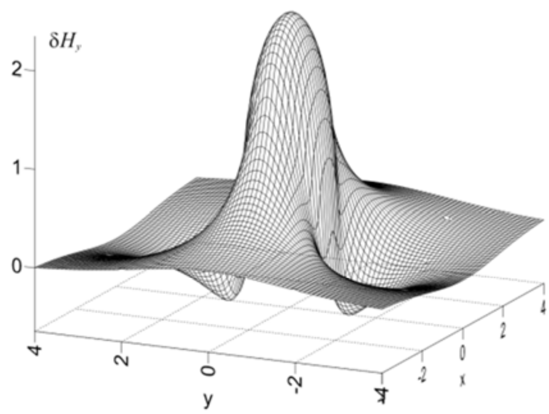

(b)

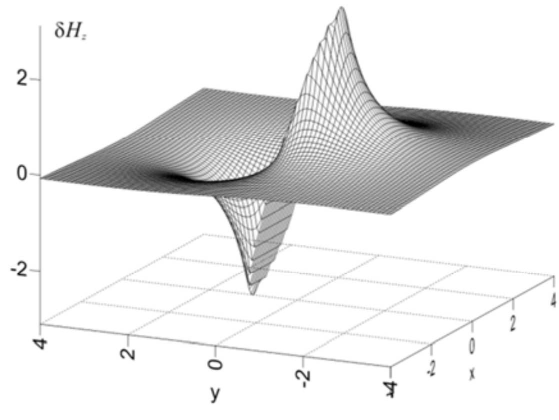

(c)

Fig. 3. *The dependences of the scattering MF components* δH_x *(a),* δH_y *(b),* δH_z *(c) on coordinates* x *and* y *for the values* $R = 1$ *,* $z = 0.001$ *. The MF values are plotted along the* Oz *axis in* j_0/c *units for the Gaussian system of units, and in* $j_0/4\pi$ *– for SI.*

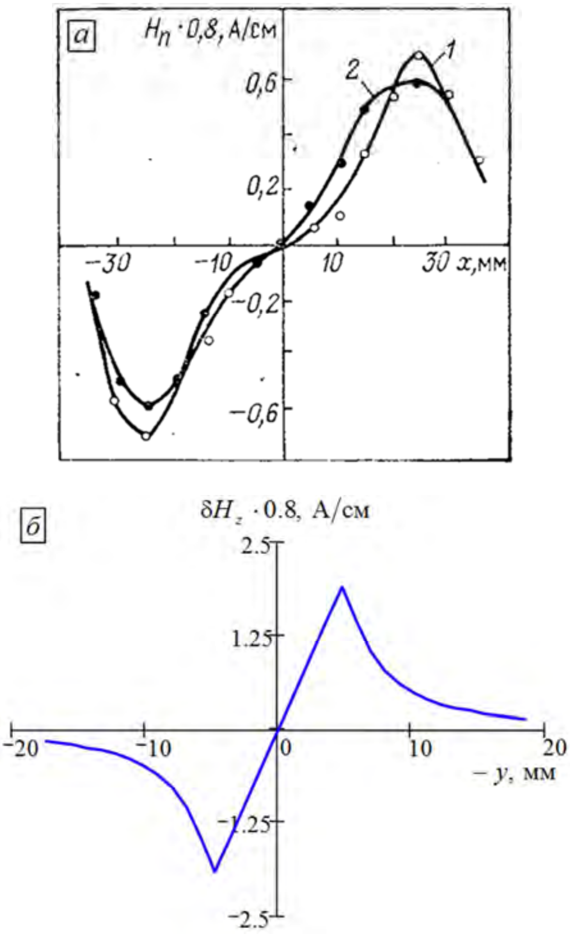

Fig. 4. *a) The dependence of the normal field component above the gap on the coordinate perpendicular to the current (gap width is 0.5 mm; depth is 4 mm; length is 60 mm) for: 1 – direct current; 2 – alternating current (experiment in [15]). b) The dependence of the normal component of the scattering MF for the surface defect in the form of a hemisphere on the coordinate perpendicular to the current (* $j_0 = 20\,\mathrm{A/см^2}$ *,* $R \approx 5$ *mm ,* $z = 0.01 \cdot R$ *).*

In Figs. 4a, 5a the obtained dependences for the MF above the gap on one of the coordinates in the plane of a sample at a fixed other coordinate and fixed distance from the sample. In Fig.4a the field components perpendicular to the surface of the sample are presented. In Fig.5a the field components in the direction of the current are represented. In Figs. 4b, 5b we demonstrate the comparison of the dependences of the corresponding scattering MF components for the hemispherical recess.

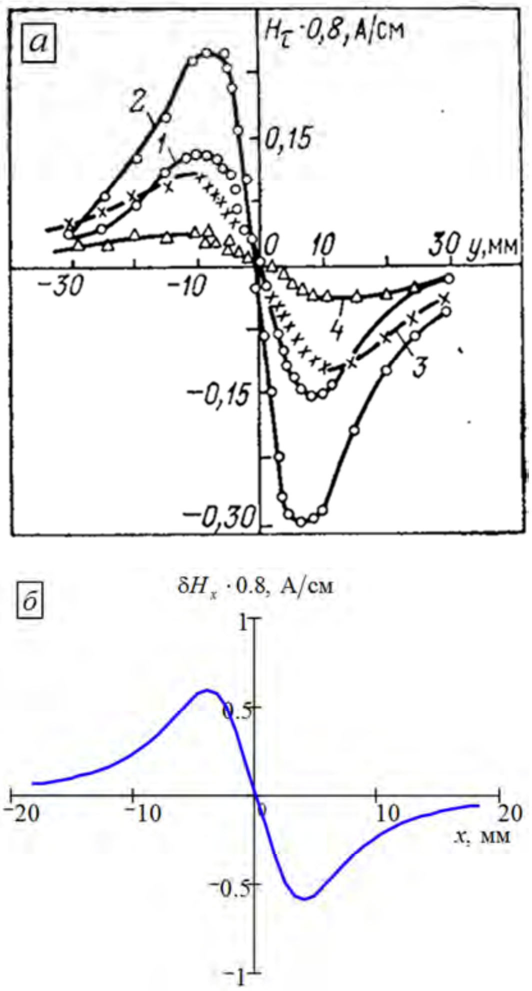

Fig. 5. *a) The dependence of the field component above the gap along the current on the coordinate parallel to the current (gap width is 0.5 mm; depth is 4 mm; length is 60 mm) for: 1 –* $x = 15\,mm$ *; 2 –* $x = 30\,mm$ *; 3 –* $x = 37\,mm$ *; 4 –* $x = 48\,mm$ *(experiment in [15]). b) The dependence of the scattering MF component along the current for the surface defect in the form of a hemisphere on the coordinate parallel to the current (* $j_0 = 20\,\mathrm{A}/\mathrm{см}^2$ *,* $R \approx 5\,mm$ *,* $z = 0.01 \cdot R$ *).*

Despite the difference between the locations of the defects and the directions of electric current in the experiment [15, 16] and presented theoretical calculations, we note a qualitative agreement of the compared dependencies. The quantitative differences between the field components associated with mismatch of the problems geometry. The defects have a different shape, in this case the sample is regarded as a semi-infinite, in [15, 16] the plate thickness is comparable to dimensions of the gap. Also in [15, 16] it is not specified, at what distance from the surface the magnetic fields were measured (Fig. 4a and Fig. 5a).

Now, when an asymptotic behavior of the scattering MF at infinity and the dependence of the field on the defect's size are clarified, it is interesting to trace the dependence of the field topology on the defect's shape. In terms of non-destructive testing it is important to answer the question whether it is possible to restore the shape of the defect by measurements of MF distribution.

5. Surface Defect in the Form of Half of an Oblate Spheroid, Cut Along the Short Axis by a Conductor Plane

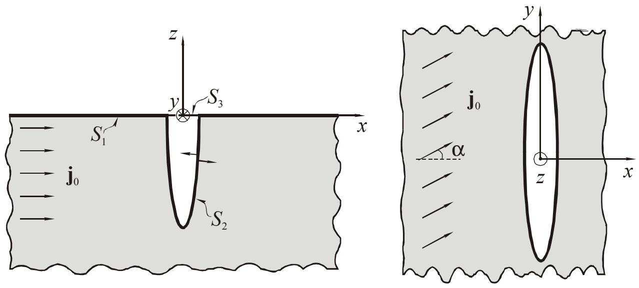

Fig. 6. *Surface defect in the form of half of an oblate spheroid, cut along the short axis. Left – side view; right – top view.*

In Sec. 4 we discussed the MF in the vicinity of a surface hemispherical defect. The form of real defects is much more complicated. Among surface defects the extended narrow slits are the most frequent [1-3].

For the defect of such a form the analytical expressions for the distributions of current density $\delta\mathbf{j}(\mathbf{r})$ and MF $\delta\mathbf{H}(\mathbf{r})$ could not be obtained.

We choose a model defect with a shape to some extent close to that of actual defects and for which an exact expression $\delta\mathbf{j}(\mathbf{r})$ could be obtained.

A cavity in the form of half of an oblate spheroid, located on the surface of the semi-infinite conductor (Fig. 6), can serve as a model for such a defect. An oblate spheroid is a figure formed by rotating an ellipse along the minor axis. It will be similar to a narrow slot if its long axis c is substantially longer than the short one a .

We choose a coordinate system with Oz axis perpendicular to the sample surface. Ox axis is directed along the minor axis of the spheroid.

Suppose that the current density vector (at infinity) is directed randomly in xOy plane. We define its orientation by angle α measured from Ox axis. Then we have

$$\phi_0 = \mathbf{j}_0\mathbf{r} = j_0 \cos\alpha \cdot x + j_0 \sin\alpha \cdot y \qquad (24)$$

Since the conductor plane divides the spheroid in half, to find the current distribution in the vicinity of the defect, it is enough to consider an equivalent problem of the current flow of a whole spheroid.

The solution of this problem is known [14]. It is compactly represented in the spheroidal coordinate system [9, 10]:

$$\mathbf{r} = \left(c_1\zeta\xi,\ \rho\cos\theta,\ \rho\sin\theta\right)$$

where $\rho = c_1\sqrt{\left(1+\zeta^2\right)\left(1-\xi^2\right)}$, $c_1 = \sqrt{c^2 - a^2}$ is the focal length, the variables ζ, ξ and θ are ranged within the corresponding limits: $0 \le \zeta < \infty$, $-1 \le \xi \le 1$, $0 \le \theta \le 2\pi$.

According to [14], the current distribution has the following form:

$$\delta\phi = j_0\cos\alpha\cdot x\cdot G_1\cdot g_1\left(\zeta\right) + j_0\cos\alpha\cdot y\cdot G_2\cdot g_2\left(\zeta\right), \quad (25)$$

$$g_1\left(\zeta\right) = \frac{1}{\zeta} - \operatorname{arctg}\frac{1}{\zeta},\quad g_2\left(\zeta\right) = \operatorname{arctg}\frac{1}{\zeta} - \frac{\zeta}{1+\zeta^2}$$

$$G_1 = \frac{ac^2}{c_1^3}\cdot\left[1 - \frac{ac^2}{c_1^3}\left(\frac{c_1}{a} - \operatorname{arctg}\frac{c_1}{a}\right)\right]^{-1}$$

$$G_2 = \frac{ac^2}{c_1^3}\cdot\left[2 - \frac{ac^2}{c_1^3}\left(\operatorname{arctg}\frac{c_1}{a} - \frac{ac_1}{c^2}\right)\right]^{-1}$$

Further, in order to calculate the scattering MF, we need to substitute the obtained current distribution in one of its calculation formulas. We use the following representation for it:

$$\delta\mathbf{H} = -\frac{1}{c}\mathbf{j}_0 \times \oint\limits_{S_2^+ + S_3} d\mathbf{S}'\frac{1}{\left|\mathbf{r}-\mathbf{r}'\right|} + \frac{1}{c}\int\limits_{S_1+S_2^-}\left[d\mathbf{S}'\times\left(\mathbf{r}-\mathbf{r}'\right)\right]\frac{\delta\phi\left(\mathbf{r}'\right)}{\left|\mathbf{r}-\mathbf{r}'\right|^3} \quad (26)$$

At the integration over the surfaces S_1, S_2^- in (26) it is necessary to put

$$d\mathbf{S}_1' = d\mathbf{S}_3' = \mathbf{e}_z\, dx'dy' = c_1^2 d\zeta d\xi\left(\zeta^2+\xi^2\right)\Big/\sqrt{\left(1+\zeta^2\right)\left(1-\xi^2\right)}$$

$d\mathbf{S}_2'^{\pm} = \pm\mathbf{e}_\zeta\, ac\sqrt{1+c_1^2\xi^2/a^2}\, d\xi d\theta = \pm\left(\mathbf{e}_x\, c^2\xi + \mathbf{e}_y\, ac\sqrt{1-\xi^2}\cos\theta + \mathbf{e}_z\, ac\sqrt{1-\xi^2}\sin\theta\right)d\xi d\theta$ and to write a distance in a spheroidal coordinate system:

$$\left|\mathbf{r}-\mathbf{r}'\right| = \sqrt{\left(x - c_1\zeta\xi\right)^2 + \left(y - c_1\sqrt{\left(1+\zeta^2\right)\left(1-\xi^2\right)}\cos\theta\right)^2 + \left(z - c_1\sqrt{\left(1+\zeta^2\right)\left(1-\xi^2\right)}\sin\theta\right)^2}$$

As a result, the expressions for each component of the scattering MF are reduced to the sum of rather cumbersome integrals. Let us present an expression only for z component:

$$\frac{c}{j_0}\cdot\delta H_z = \cos\alpha\left[I_1^{(z)}\left(\mathbf{r}\right) + I_2^{(z)}\left(\mathbf{r}\right) + I_3^{(z)}\left(\mathbf{r}\right)\right] + \sin\alpha\left[I_4^{(z)}\left(\mathbf{r}\right) + I_5^{(z)}\left(\mathbf{r}\right) + I_6^{(z)}\left(\mathbf{r}\right)\right] \quad (27)$$

$$I_1^{(z)}\left(\mathbf{r}\right) = -ac\int\limits_{\pi}^{2\pi} d\theta\int\limits_{-1}^{1} d\xi\,\frac{\sqrt{1-\xi^2}\cos\theta}{\left|\mathbf{r}-\mathbf{r}'\right|_{\zeta=a/c_1}}$$

$$I_2^{(z)}\left(\mathbf{r}\right) = -ac^2G_1g_1\left(\frac{a}{c_1}\right)\int\limits_{\pi}^{2\pi} d\theta\int\limits_{-1}^{1} d\xi\,\frac{\xi^2\left(y - c\sqrt{1-\xi^2}\cos\theta\right)}{\left|\mathbf{r}-\mathbf{r}'\right|^3_{\zeta=a/c_1}}$$

$$I_3^{(z)}\left(\mathbf{r}\right) = a^2cG_1g_1\left(\frac{a}{c_1}\right)\int\limits_{\pi}^{2\pi} d\theta\int\limits_{-1}^{1} d\xi\,\frac{\xi\sqrt{1-\xi^2}\cos\theta\left(x - a\xi\right)}{\left|\mathbf{r}-\mathbf{r}'\right|^3_{\zeta=a/c_1}}$$

$$I_4^{(z)}\left(\mathbf{r}\right) = c^2\int\limits_{\pi}^{2\pi} d\theta\int\limits_{-1}^{1} d\xi\,\frac{\xi}{\left|\mathbf{r}-\mathbf{r}'\right|_{\zeta=a/c_1}}$$

$$I_5^{(z)}\left(\mathbf{r}\right) = -c^3G_2g_2\left(\frac{a}{c_1}\right)\int\limits_{\pi}^{2\pi} d\theta\int\limits_{-1}^{1} d\xi\,\frac{\xi\sqrt{1-\xi^2}\cos\theta\left(y - c\sqrt{1-\xi^2}\cos\theta\right)}{\left|\mathbf{r}-\mathbf{r}'\right|^3_{\zeta=a/c_1}}$$

$$I_6^{(z)}\left(\mathbf{r}\right) = ac^2G_2g_2\left(\frac{a}{c_1}\right)\int\limits_{\pi}^{2\pi} d\theta\int\limits_{-1}^{1} d\xi\,\frac{\left(1-\xi^2\right)\cos^2\theta\left(x - a\xi\right)}{\left|\mathbf{r}-\mathbf{r}'\right|^3_{\zeta=a/c_1}}$$

To calculate these integrals we can use the expansion of the inverse distance in spheroidal harmonics [9, 10].

Let us proceed differently: we calculate the MF components numerically.

In Fig. 7 we present the dependences of the scattering field components on coordinates in the plane of the sample at the parallel and perpendicular orientations of the current vector $\mathbf{j}_0$ (at infinity) with respect to the short axis of the spheroid. The ratio between the axes is $a/c = 1/10$.

The isolines presented in Fig. 8 give a qualitative picture of the distribution of MF components in accordance with the dependences in Fig. 7.

It follows from the analysis of these figures that, basing on the distribution of MF over a defect, we can obtain the information not only about its location and orientation of the defect in the sample, but also about the relationship between its transverse and longitudinal dimensions.

To estimate the depth of the defect is necessary to measure the value of MF at different distances from the surface of the conductor. Besides, an additional information about the defect could be obtained by measuring variable fields at different frequencies of the primary EMF. However, to solve the latter problem it is necessary to determine not an approximate but an exact distribution of MF at an arbitrary depth of the skin layer.

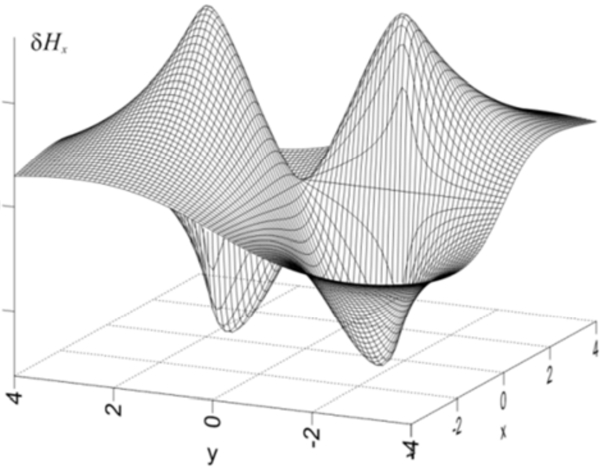

(a1)

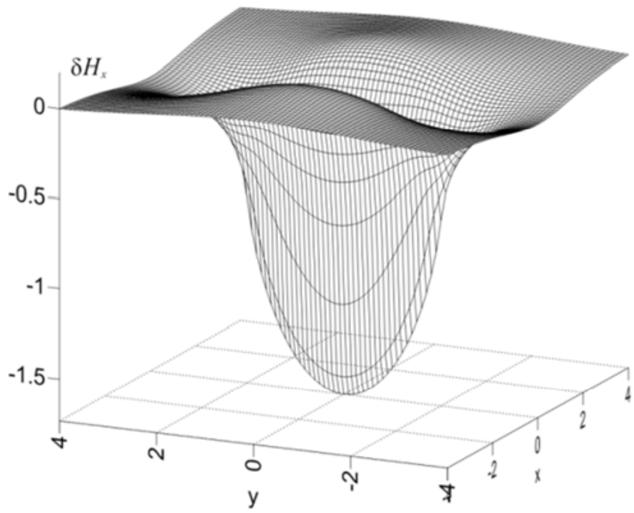

(a2)

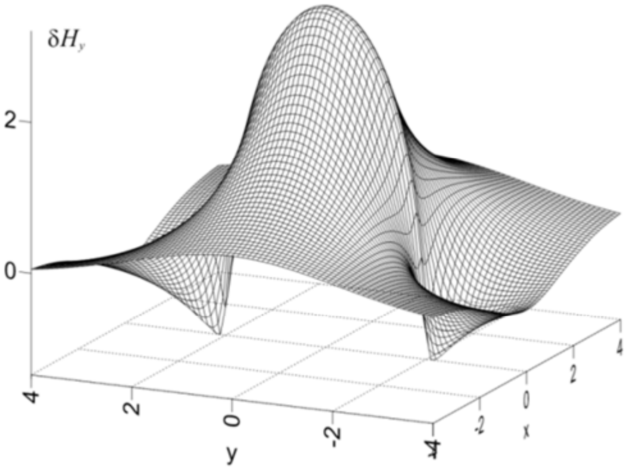

(b1)

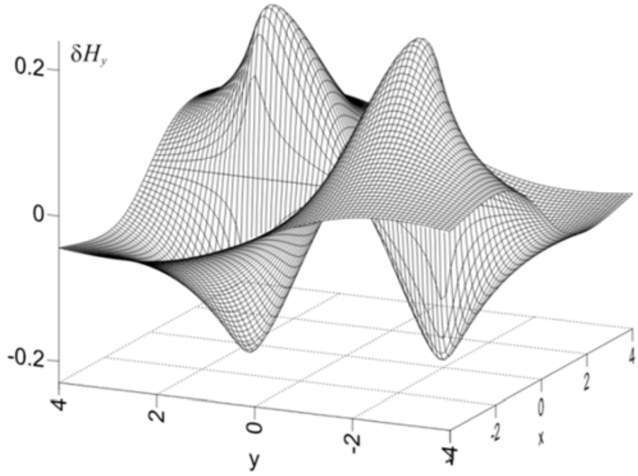

(b2)

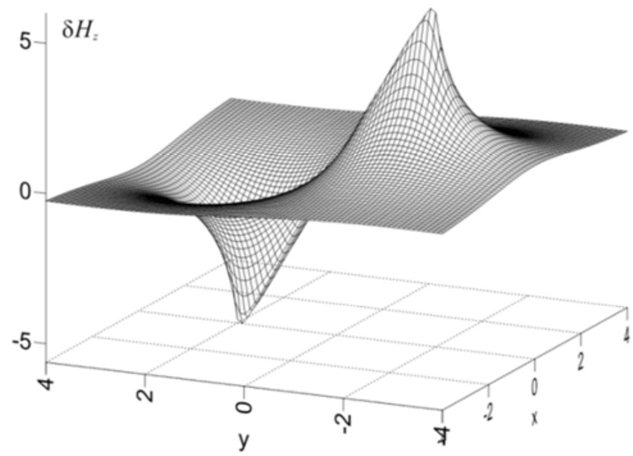

(c1)

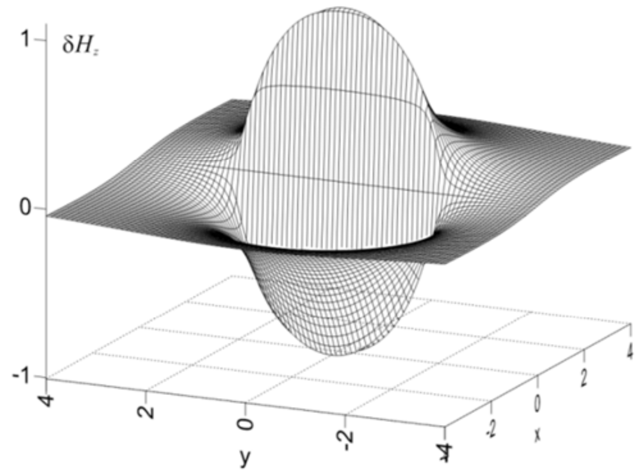

(c2)

Fig. 7. *The dependences of the scattering MF components: a1, a2)* δH_x *; b1, b2)* δH_y *; c1, c2)* δH_z *on* x *and* y *coordinates for* $a = 0.2$, $c = 10a$, $z = 0.1a$ *. The index 1 corresponds to* $\alpha = 0$ *, index 2 – to* $\alpha = \pi/2$ *.* $z = 0.001$ *. The values of MF are plotted along Oz axis in* j_0/c *units for the Gaussian system of units, and in* $j_0/4\pi$ *– for SI.*

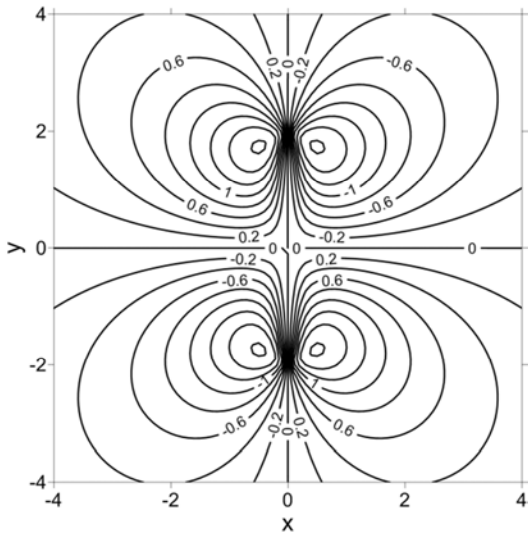

(a1)

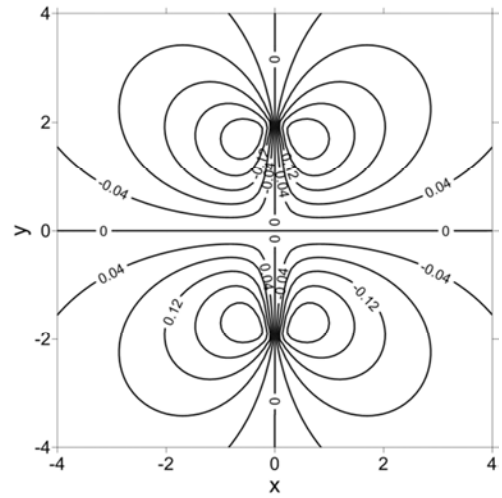

(b2)

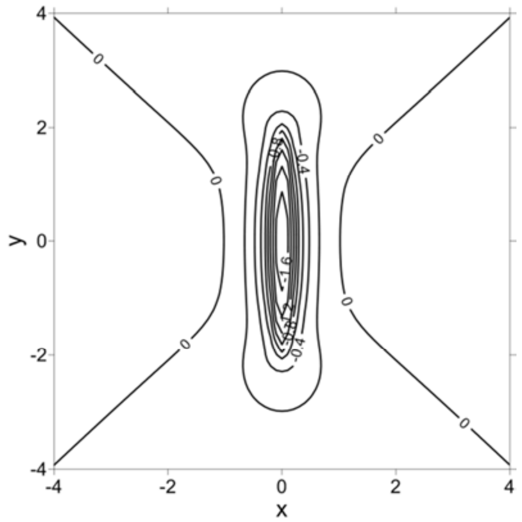

(a2)

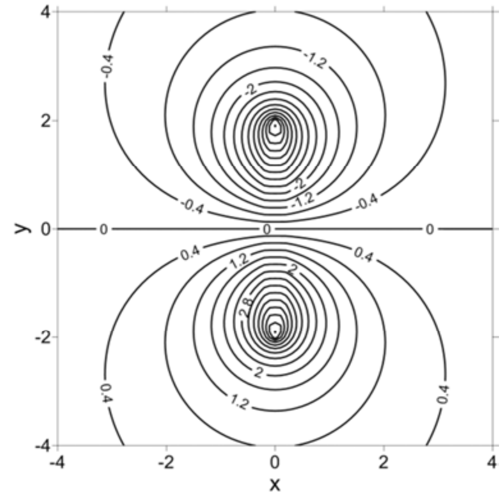

(c1)

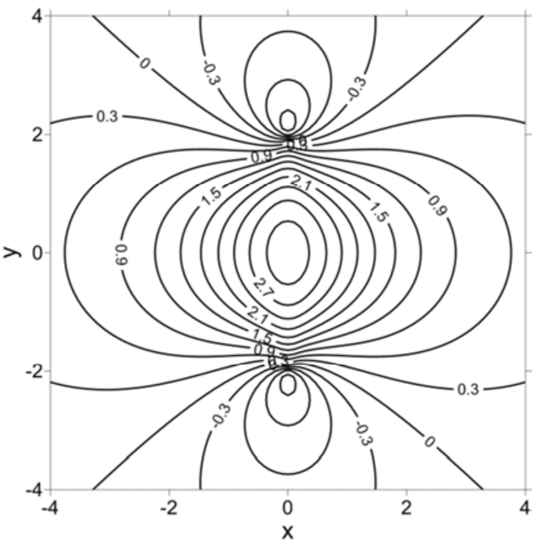

(b1)

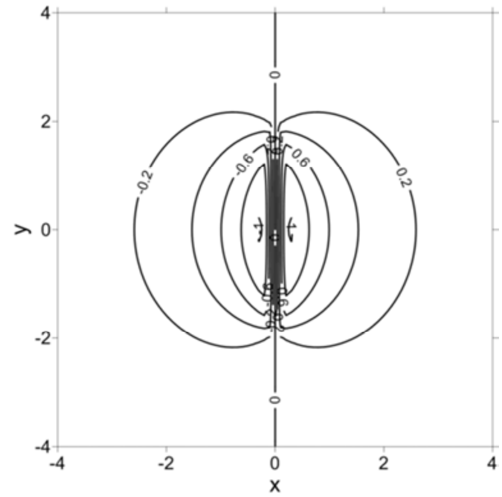

(c2)

Fig. 8. *The isolines of scattering MF components: a1, a2)* δH_x *; b1, b2)* δH_y *; c1, c2)* δH_z *for* $a = 0.2$ *,* $c = 10a$ *,* $z = 0.1a$ *. The index 1 corresponds to* $\alpha = 0$ *, index 2 – to* $\alpha = \pi/2$ *. The values of MF are referred to* j_0/c *for the Gaussian system of units, and to* $j_0/4\pi$ *– for SI.*

References

[1] R. I. Janus, *Magnetic Defectoscopy*, Moscow, Leningrad, Gostekhizdat, 1946 [in Russian].

[2] N. N. Zatsepin and L. V. Korzhova, *Magnetic Defectoscopy*, Minsk, Science and Technology, 1981 [in Russian].

[3] A. L. Dorofeev, *Non-destructive Testing by the Eddy Currents Method*, Moscow, Oborongiz, 1961 [in Russian].

[4] H. G. Ramos, T. Rocha, A. L. Ribeiro, and D. Pasadas, *GMR versus differential coils in velocity induced eddy current testing*, Proceedings of IEEE International Instrumentation and Measurement Technology Conference (I2MTC), 2014.

[5] A. L. Ribeiro, D. Pasadas, H. G. Ramos, and T. Rocha, *Using Excitation Invariance in the Characterization of Defects by Eddy Current Image Constructions*, Proc. International Conf. on Structural Integrity (ICONS), Kalpakkam, India, 2014.

[6] H. G. Ramos, T. Rocha, A. L. Ribeiro, and D. Pasadas, *Determination of Linear Defect Depths from Eddy Currents Disturbances*, Proc. Review of Progress in Quantitative Nondestructive Evaluation (QNDE), Baltinore, United States, 2013.

[7] L. D. Landau and E. M. Lifshitz, *Electrodynamics of Continuous Media*, Moscow, Nauka, 1982 [in Russian].

[8] V. Smite, *Electrostatics and Electrodynamics*, Moscow, Inostrannaya Literatura, 1954 [in Russian].

[9] F. M. Morse and H. Feshbach, *Methods of Theoretical Physics*, Vol. 1-2, Moscow, Inostrannaya Literatura, 1958 [in Russian].

[10] R. Courant and D. Hilbert, *Methods of Mathematical Physics*, Vol. 1-2, New York, Interscience Publishers, 1937.

[11] ASM Handbook. Formerly Ninth Edition, Metals Handbook, Vol. 17. *Non-destructive Evaluation and Quality Control*, ASM International, p. 136-142.

[12] L. D. Landau and E. M. Lifshitz, *Fluid Mechanics*, Moscow, Nauka, 1986 [in Russian].

[13] G. Lamb, *Hydrodynamics*, Cambridge, Cambridge University Press, 1932.

[14] N. E. Kochin, I. A. Kibel, N. V. Rose, *Theoretical Hydromechanics*, Parts I and II, Moscow, State Publisher of Physical and Mathematical Literature, 1963 [in Russian].

[15] N. N. Zatsepin and N. P. Benklevskaya, Russian Journal of Nondestructive Testing, Vol. 5, P. 103-112 (1969).

[16] N. N. Zatsepin and N. P. Benklevskaya, Russian Journal of Nondestructive Testing, Vol. 6, P. 89-94 (1970).